

1 **Title:** Organic layers preserved in ice patches: A new record of Holocene environmental change
2 on the Beartooth Plateau, USA.

3

4 **Authors:** Alt, Mio¹, Puseman, Kathryn², Lee, Craig M.³, Pederson, Gregory T.⁴, McConnell,
5 Joseph R.⁵, Chellman, Nathan J.⁵, McWethy, David B.¹

6

7 **Affiliations:**

8 ¹Department of Earth Sciences, Montana State University, Bozeman, MT 59717, USA

9 ²Paleoscapes Archaeobotanical Services Team, LLC, Bailey, Colorado 80421

10 ³Department of Sociology & Anthropology, Montana State University, Bozeman, MT 59717

11 ⁴U.S. Geological Survey, Northern Rocky Mountain Research Station, Bozeman, MT 59717

12 ⁵Division of Hydrologic Sciences, Desert Research Institute, Reno, Nevada 89512

13

14 **Corresponding Author:**

15 Mio Alt

16 Mio.alt1@montana.edu

17

18

19

20

21

22

23

24

25

26

27

28

29

30

31

32 **Abstract**

33

34 Growing season temperatures play a crucial role in controlling treeline elevation at
35 regional to global scales. However, understanding of treeline dynamics in response to long-term
36 changes in temperature is limited. In this study, we analyze pollen, plant macrofossils, and
37 charcoal preserved in organic layers within a 10,400-year-old ice patch and in sediment from a
38 6,000-year-old wetland located above present-day treeline in the Beartooth Mountains,
39 Wyoming, to explore the relationship between Holocene climate variability and shifts in treeline
40 elevation. Pollen data indicate a lower-than-present treeline between 9000-6200 cal yr BP during
41 the warm, dry summer and cold winter conditions of the early Holocene. Increases in arboreal
42 pollen at 6200 cal yr BP suggest an upslope treeline expansion when summers became cooler
43 and wetter. A possible hiatus in the wetland record at ca. 4200-3000 cal yr BP suggests increased
44 snow and ice cover at high elevations and a lowering of treeline. Treeline position continued to
45 fluctuate with growing season warming and cooling during the late Holocene. Periods of high
46 fire activity correspond with times of increased woody cover at high elevations. The two records
47 indicate that climate was an important driver of vegetation and treeline change during the
48 Holocene. Early Holocene treeline was governed by moisture limitations, whereas late-Holocene
49 treeline was sensitive to increases in growing season temperatures. Climate projections for the
50 region suggest warmer temperatures could decrease effective growing season moisture at high
51 elevations resulting in a reduction of treeline elevation.

52

53 **Key Words:** alpine treeline, pollen analysis, ice patches, vegetation change, Rocky Mountains,
54 Holocene

55

56 **Introduction**

57

58 Ecosystems throughout the western U.S. are responding to rapid warming, and evidence
59 suggests some alpine environments are warming at greater rates than lowland environments
60 (Pepin et al., 2015). Ecosystem models predict latitudinal and altitudinal shifts in treeline with
61 warming temperatures (Lenoir et al., 2008), although local site conditions potentially complicate
62 the specific trajectories of change (Quadri et al., 2021). For example, subalpine forests that

63 become moisture-limited could decline rather than exhibit an expected positive growth and
64 recruitment response to warming temperatures (Andrus et al., 2018). The current rate of climatic
65 changes driving high-elevation ecosystems towards possible extinction events related to
66 mountaintop bioclimatic envelope ‘traps’ (Rehm and Feeley, 2016) highlights a need to better
67 understand the magnitude of paleoclimatic and paleoecological changes, as well as their effect on
68 subalpine treeline. Additionally, records focusing on how subalpine treeline position has
69 fluctuated across multiple timescales may clarify whether temperature or moisture acts as the
70 primary drivers of change.

71 Warming temperatures are causing rapid melting of perennial ice patches in alpine
72 environments worldwide, exposing organic debris and cultural materials that have been
73 preserved in ice for millennia. Ice Patch Archaeology has grown in response, shedding new light
74 on the human use of high-elevation landscapes (Lee, 2012; Lee and Puseman, 2017). Though the
75 interest in ice patches primarily has been archaeological, work has been done to understand how
76 the development of ice patches relates to climate conditions (Meulendyk et al., 2012). Recent
77 efforts also have sought to uncover paleoclimatic information from within the ice, aided by the
78 presence of organic sediment layers which allow for radiocarbon-based age-depth estimates
79 (Chellman et al., 2021).

80 Across the northern Rocky Mountains, numerous ice patches are situated near and above
81 modern treeline. Although some of these patches have persisted for millennia, under current
82 climatic conditions, many are shrinking in volume or disappearing altogether. In concert with
83 their location at high elevations, the information they contain provides us with a unique but at-
84 risk opportunity to examine high-elevation paleoenvironments typically not captured by
85 traditional paleoecological methods. Chellman et al. (2021) reconstructed cool-season
86 temperature and moisture for the last 10,400 years from an ice patch (named TL1) on the
87 Beartooth Plateau of northwestern Wyoming, within the Greater Yellowstone Ecosystem (GYE).
88 Unlike other records from alpine glaciers, the Beartooth TL1 Ice Patch record was not impacted
89 by ice thinning, and the chronology was well-constrained by 29 radiocarbon dates obtained from
90 organic layers relatively evenly distributed throughout the ice profile. These layers not only
91 provide unparalleled opportunities to develop age-depth chronologies, but also to examine
92 macrofossils, pollen, and charcoal to reconstruct the environmental conditions associated with
93 the time intervals when the organic layers formed.

94 The postglacial vegetation history of the GYE has been described through the analysis of
95 pollen, charcoal, and diatoms from lakes and wetlands (Huerta et al., 2009; Iglesias et al., 2018;
96 Krause et al., 2015; Krause and Whitlock, 2013; Millspaugh et al., 2000; Whitlock, 1993;
97 Whitlock et al., 2012), yet records obtained from alpine settings exploring the subalpine forest to
98 alpine tundra ecotone are more scarce (Fall et al., 1995; Lynch, 1996; Rust and Minckley, 2020).
99 Ice patches above treeline offer an opportunity to investigate elevation shifts and fluctuations in
100 the composition and density of subalpine forests (Benedict, 2011; Benedict et al., 2008). Present-
101 day treeline is a harsh environmental setting where upslope/downslope shifts are likely governed
102 by variations in climate and local site conditions. At large spatial scales (subregional to
103 continental), the location of subalpine treeline is associated most strongly with growing season
104 temperature (Harsch and Bader, 2011; Hoch and Körner, 2009; Körner and Paulsen, 2004).
105 Although growing season temperature is a dominant factor, local treeline position also is
106 mediated by moisture availability, wind, avalanches, slope, aspect, topography, and disturbance
107 (Andrus et al., 2018; Schwörer et al., 2017).

108 Here, we set out to develop an understanding of subalpine climate and treeline dynamics
109 (e.g., changes in elevation, species composition, and structure) during the Holocene (i.e., the last
110 12,000 years) by: 1) analyzing pollen, charcoal, and macrofossils from organic layers in ice cores
111 from the Beartooth TL1 Ice Patch and in sediment cores from an adjacent wetland, Meltwater
112 Pond, on the Beartooth Plateau, WY, 2) comparing the information contained within the two
113 records, 3) discussing the similarities and differences between these proxies and what processes
114 drive the accumulation of organic layers, 4) evaluating these new paleoenvironmental records in
115 the context of published $\delta^{18}\text{O}$ and ice accumulation records from the same ice patch (Chellman et
116 al., 2021), as well as with other records across the Greater Yellowstone Ecosystem and northern
117 Rocky Mountains.

118

119 ***Study site***

120

121 The Beartooth Plateau is an expansive high-elevation peneplain in the Beartooth
122 Mountain Range, located in south-central Montana and northwest Wyoming, reaching elevations
123 up to 3900 masl. The two sites in this study, Beartooth TL1 Ice Patch (hereafter referred to as
124 TL1; 3145 masl) and Meltwater Pond (MP; 3090 masl) are located in a glacially carved basin on

125 the Beartooth Plateau (Fig. 1). TL1 is situated on the southwest wall of the basin and was a 215 x
126 120 m ellipsoidal patch at the time of coring (Chellman et al., 2021). At the time of coring, MP
127 was .07 ha and had a maximum water depth of 1 m. The water in MP largely originates from
128 melting upland snow, the amount of which can alter the size and depth of the pond. The west
129 side of the pond has a wetland margin.

130 Vegetation in the Beartooth Mountain Range is arrayed by elevation. *Pinus flexilis*
131 (limber pine) and *Pseudotsuga menziesii* (Douglas-fir) forests are prevalent at elevations
132 between 1700-2500 masl, *Pinus contorta* (limber pine) forests are found at 2000-2800 masl, and
133 *Abies lasiocarpa* (subalpine fir) subalpine forests dominate elevations between 2500-3000 masl,
134 although *Picea engelmannii* (Engelman spruce) forests are found in cold and wet sites (Pfister et
135 al., 1977; Williams, 2012). *Pinus albicaulis* (whitebark pine) forests are found at the highest
136 elevations between 2500-3000 masl, and stunted *Pinus albicaulis*, *Abies lasiocarpa*, and *Picea*
137 *engelmannii* occur in krummholz patches above upper forest treeline between 3000-3200 masl
138 (Williams, 2012). Above treeline (approximately 3000 masl), alpine tundra includes species of
139 Poaceae (e.g., *Poa alpina* and *Festuca brachyphylla*), *Carex* (e.g., *C. rupestris*, *C.*
140 *phaeocephala*, *C. scopulorum*, and *C. nigricans*), *Salix* (e.g., *S. reticulata* and *S. glauca*), and
141 *Artemisia* (*A. scopulorum* and *A. tridentata*), as well as other small shrubs and herbaceous
142 vegetation (e.g., *Dryas octopetala*, *Geum rossii*, *Phlox caespitosa*, *Polygonum bistortoides*,
143 *Potentilla diversifolia*, *Gentiana algida*, and *Phyllodoce empetriforims*; Heidel et al., 2017;
144 Williams, 2012)

145 The alpine-parkland ecotone in the TL1 and MP basin is diffuse with an approximate
146 upper elevation of ~3050 m asl, about 0.6 km away from TL1 and MP. The closest subalpine
147 forest stand is located ~1 km away from the two sites at ~3000 m asl. Vegetation immediately
148 surrounding the sites include grasses, sedges, shrubs, and herbs typical of alpine tundra (as listed
149 above).

150 Interpolated climate normals for 1991-2020 indicate temperatures are highest in July
151 (average of 12°C) and lowest in December (average of -9.5°C), with an average annual
152 temperature of -0.1°C (PRISM Climate Group, 2022). The high-elevation parts of the basin
153 receive an average of ~800 mm of annual precipitation, most of which is received as snow in the
154 winter and spring months (DJF=175 mm, MAM=275 mm), and least in the summer months
155 (JJA=165 mm; PRISM Climate Group, 2022). Cool season precipitation comes from westerly

156 storm tracks originating over the Pacific Ocean. A secondary spring precipitation pulse also
157 delivers substantial amounts of moisture to the region from regional recycling of winter moisture
158 and upsloping easterlies laden with moisture advected from the Gulf of Mexico (Wise et al.,
159 2018). Spring precipitation events occur in the form of convectional storms or snowfall at high
160 elevations. Late summer is typically dry due to the influence of the Pacific subtropical high-
161 pressure system, which suppresses precipitation in the northern Rocky Mountains (Whitlock and
162 Bartlein, 1993).

163

164 [Insert Figure 1]

165

166 **Methods**

167

168 *Field*

169

170 Three ice cores were recovered from the TL1 Ice Patch in 2016, using a 4" diameter
171 "PrairieDog" two-barreled ice coring device (Kyne and McConnell, 2007; for more information
172 on ice core methods see Chellman et al., 2021). The longest ice core was 5.61 m in length and
173 contained 29 layers of organic sediment (henceforth termed "organic layers"), ranging in
174 thickness from 0.5-4 cm. The organic layers were isolated by a hand saw, bagged in the field,
175 and refrigerated until analysis. In 2022, a sample of the organic matter deposited on the surface
176 of the TL1 was collected and refrigerated until analysis.

177 In 2018, two 100-cm sediment cores were retrieved using a Russian Peat coring device
178 from the wetland margin of Meltwater Pond, where sediments were the deepest. In 2022, surface
179 samples from the wetland were collected. Cores and the surface samples were wrapped in plastic
180 wrap and aluminum foil and stored in the cold storage room at Montana State University until
181 analysis.

182

183 *Lithology and chronology*

184

185 The 29 organic layers from the longest TL1 core were inspected, and material from each
186 layer was sent to the AMS Radiocarbon Preparation and Research facility in Boulder, CO for

187 accelerated mass spectrometry (AMS) radiocarbon dating (for more information see Chellman et
188 al., 2021). The lithology of the MP core was described, and because no macrofossils were found
189 in the core, six bulk sediment samples were submitted to the NOSAMS Woods Hole
190 Oceanographic Institute for AMS radiocarbon dating. The AMS radiocarbon ages were
191 converted to calibrated ages using CALIB Radiocarbon Calibration Program 8.2 (Stuiver and
192 Reimer, 1993). Age-depth models for both the TL1 and MP were created using the BACON
193 software, which utilizes a Bayesian statistical approach to reconstruct accumulation rates
194 (Blaauw and Christen, 2011). While the processes driving the deposition of layers of ice in the
195 ice patch differ from those responsible for sediment accumulation in the wetland, the approach
196 for developing the well-dated chronology associated with the ice patch age-depth model is
197 supported by multiple lines of evidence indicating that thin layers of ice and organic material
198 accumulated chronologically as discussed in detail in Chellman et al. 2021.

199

200 *TL1 Ice Patch macrofossil analysis*

201

202 The organic samples from the ice core were rinsed through chiffon fabric, dried, and
203 weighed. They were screened using a series of graduated screens (US Standard Sieves with 4-
204 mm, 2-mm, 1-mm, 0.5-mm, and 0.25-mm openings), and the contents of each screen were
205 examined under a Stereozoom microscope at magnifications of 10-70x. Some charcoal
206 specimens also were examined using magnifications of 100-600x. Macrofloral remains were
207 recorded as charred and/or uncharred, whole and/or fragments using counts, weights, and/or
208 frequencies. Macrofloral remains and charcoal fragments were identified to the lowest taxonomic
209 level possible using standard identification manuals (Cappers and Bekker, 2013; Carlquist, 1988;
210 Core et al., 1976; Delorit, 1970; Hoadley, 1990; Knobel, 1980; Martin and Barkley, 2000;
211 Panshin and deZeeuw, 1980), databases (InsideWood, 2004; Schweingruber and Landolt, 2005)
212 and a modern comparative collection.

213

214 *Pollen analysis*

215

216 The TL1 surface sample, sediment from 15 of the organic layers, and sediment from 25
217 sections of the MP core were processed for pollen following standard procedures (Bennett and

218 Willis, 2001). A *Lycopodium* tracer was added to each sample to calculate pollen concentration
219 (grains/cm³) and accumulation rates (grains/cm²/yr). A minimum of 300 pollen grains was
220 counted at 400-1000x magnification and identified to the lowest possible taxonomic level using
221 reference collections at Montana State University and pollen manuals (McAndrews et al, 1973;
222 Faegri and Iverson, 1989; Kapp et al., 2000). Pollen results were separated into stratigraphic
223 zones designated through cluster analysis performed by the CONISS program (Grimm, 1987).
224 Tree species (*Populus* sp., *Tsuga heterophylla*, *Juniperus* sp., and *Pseudotsuga menziesii*) and
225 several upland herb species that were present in small percentages (<1%) were grouped into
226 “other trees” and “other shrubs and herbs” categories. Arboreal pollen (AP) represents all trees
227 and shrubs other than *Artemisia*, and non-arboreal pollen (NAP) includes *Artemisia*, all herbs,
228 and grasses. The AP:NAP ratio was calculated as (AP-NAP/AP+NAP).

229

230 *Charcoal analysis*

231

232 For the TL1 organic layers, microscopic charcoal was counted on the pollen slides and
233 converted to concentration, and macroscopic charcoal particles were counted as described above
234 in the TL1 macrofossil analysis section. For the MP core, contiguous sediment samples of 2 cm³
235 at 1-cm intervals were processed following the procedures outlined by Whitlock and Larsen
236 (2001), and particles (> 125 µm) were counted under a stereomicroscope. Charcoal counts were
237 converted to charcoal accumulation rates (CHAR), and fire events and changes in fire frequency
238 over time were identified using the CharAnalysis software for MatLab (Higuera et al., 2009).
239 Background charcoal accumulation rates (BCHAR) were calculated using a 900-year lowess
240 smoother, which optimized the signal-to-noise ratio (Kelly et al., 2011).

241

242 **Results**

243

244 **TL1 Ice Patch**

245

246 *Lithology*

247 The 29 organic layers consisted of organic detritus, small gravel, degraded plant
248 macrofossils, and herbivore digesta (plant material digested by herbivores). The thickness of the

249 deposits varied from 0.5-4 cm, and weights varied between 0.015 g and 317.6 g (Table 1). The
 250 heaviest layers (>2 g) were numbers 1, 3, and 4 (deposited between ca. 940-2436 cal yr BP), 17
 251 (ca. 5800 cal yr BP), 21 (ca. 7800 cal yr BP), and 27-29 (ca. 9600-10400 cal yr BP). The lightest
 252 layers (<1 g) were layers 15 and 16 (ca. 5488-5993 cal yr BP), 22 and 23 (ca. 8994-9020 cal yr
 253 BP), 25 and 26 (ca. 8994-9180 cal yr BP), and a long sequence between layers 5 and 13 (ca.
 254 2800-5100 cal yr BP). The heaviest sample (layer 29 at the base of the ice core), consisted of
 255 numerous small pieces of gravel.

256

257 *Chronology*

258 The age-depth model for the TL1 core was based on 29 AMS radiocarbon dates from
 259 organic material (e.g., seeds, leaves, twigs) from each of the organic layers (Table 1; SM Fig. 1).
 260 See Chellman et al., 2021 for more information on the age-depth chronology. The deepest
 261 organic layer dated to 10,333-10,415 cal yr BP (1 σ uncertainty), and the most recent layer at a
 262 depth of 166 cm dated to 945-955 cal yr BP (1 σ uncertainty).

263

264 **Table 1.** TL1 Ice Patch sediment depths, ages, and weights.

Lag Number	Depth (cm)	Uncalibrated Age (^{14}C yr BP)	Calibrated Age Range (Cal yr BP)(Probability)	Sample Weight (g)
1	166	1,025 ± 15	945-955(.56)	11.888
2	216	1,790 ± 15	1633-1658(.64)	1.416
3	255	2,060 ± 15	2022-2044(.47)	3.444
4	272	2,465 ± 15	2636-2698(.60)	3.474
5	298	2,715 ± 20	2816-2847(.55)	0.694
6	314	2,850 ± 20	2930-2997(.90)	0.967
7	321	3,540 ± 20	3827-2873(.66)	0.147
8	325	3,005 ± 20	3162-3229(1.0)	0.594
9	371	3,220 ± 20	3401-3429(.70)	0.548
10	381	3,680 ± 20	4033-4082(.69)	0.047
11	392	4,030 ± 20	4440-4487(.76)	0.714
12	396	4,175 ± 20	4700-4739(.42)	0.015
13	410	4,500 ± 20	5053-5142(.60)	0.385
14	415	5,340 ± 20	6114-6147(.36)	1.488
15	422	4,825 ± 20	5488-5504(.51)	0.104
16	431	5,220 ± 20	5959-5993(.69)	0.155
17	433	5,185 ± 20	5917-5938(.64)	16.413
18	442	5,460 ± 20	6276-6292(.55)	0.278
19	449	5,980 ± 25	6810-6853(.55)	1.511
20	472	6,095 ± 25	6933-6994(.81)	0.495
21	484	7,165 ± 25	7964-8009(1.0)	19.699
22	512	8,085 ± 25	8994-9023(1.0)	0.444
23	529	8,065 ± 25	8987-9020(1.0)	0.168
24	537	8,045 ± 25	8982-9012(.62)	1.689
25	539	8,080 ± 25	8994-9020(1.0)	0.582
26	542	8,255 ± 25	9137-9180(.36)	0.556
27	555	8,725 ± 25	9598-9710(.88)	2.754
28	557	8,765 ± 25	9688-9784(.74)	2.299
29	560	9,215 ± 25	10333-10415(.64)	317.601

265

266

267 *Pollen, charcoal, and macrofossils*

268 The TL1 record was divided into 5 zones based on a constrained cluster analysis of the
269 pollen percentages (Grimm, 1987; Fig. 2). Zone IP1 (layers 29-24; ca. 10,400-8500 cal yr BP)
270 had the highest levels of *Pinus* pollen of the record at the very base (48%), as well as moderate
271 amounts of *Picea* (5%), although both pollen species declined towards the top of the zone (to
272 21% and 2%, respectively). Poaceae levels were low in the deepest sample (5%), but quickly
273 rose (to 50%). *Artemisia* pollen levels were moderate (15%), and *Selaginella* levels increased
274 (from 5% to 10%) towards the top of the zone. The arboreal pollen to nonarboreal pollen ratio
275 (AP:NAP) declined from the highest of the record at the very base to the lowest of the record
276 near the top of the zone. Numerous Poaceae parts (stems, leaves, florets, and caryopses),
277 *Potentilla* seeds, and unidentified leaf fragments were found in each layer, as well as seeds and
278 perigynia of *Carex* species favoring both wetlands (*C. capitata*, *C. illota*, *C. scirpoidea*), and
279 high-elevation rocky outcrops (*C. albonigra*, *C. elynoides*, and *C. haydeniana*). *Picea* needles
280 were found in layers 27-29, as well as a Pinaceae seed wing in layer 29 (SM Fig. 2).
281 Microcharcoal concentrations were high at the base, and decreased to the top of the zone,
282 suggesting a decrease in fire activity.

283 Zone IP2 (layers 21-19; 8500-6500 cal yr BP) was characterized by low AP:NAP levels,
284 including low amounts of *Pinus* pollen (25-35%), as well as the least amount of *Picea* pollen of
285 the record (2-4%). *Artemisia* values increased through the zone (26-29%), and Poaceae levels
286 declined (21-11%), suggesting an open sagebrush steppe or tundra landscape. A few *Picea*,
287 *Abies*, and *Pinus* needle fragments were found in layer 21. Poaceae parts (stems, leaves, florets,
288 and caryopses) and *Carex* seeds and perigynia were still present, as well as *Potentilla* seeds.
289 Microscopic charcoal concentrations decreased in this zone, indicating low fire activity.

290 Zone IP3 (layers 18-14; 6500-4900 cal yr BP) was characterized by lower levels of
291 *Artemisia* (10-15%) than before, and high levels of Poaceae (35-45%), except for layer 16,
292 which had a low percentage of Poaceae (11%). *Pinus* and *Picea* levels increased from Zone IP2
293 (25-42% and 4-7% respectively), as did Rosaceae (2-10%). AP:NAP was high in layer 16, and
294 although layers 18 and 14 were below average, they were higher than the AP:NAP in Zone IP2,
295 indicating that forest density increased. Microscopic charcoal concentrations also increased in
296 this zone, indicating more fire activity than in Zone IP2.

297 Zone IP4 (layers 11-6; 4900-2800 cal yr BP) was characterized by an increase of *Pinus*
298 (37-39%) and *Picea* (4-8%), an increase in *Artemisia* (11-27%), and a decrease in Poaceae pollen
299 (27-11%). Caryophyllaceae values increased, as did those of other shrubs and herbs. Poaceae
300 macrofossils (stems, leaves, and florets), *Potentilla* seeds, and Cyperaceae seeds and perigynia
301 continued to be present throughout the zone, and there was one *Pinus* needle found in layer 6.
302 Brassicaceae seeds also were abundant. AP:NAP increased in this zone, and microscopic
303 charcoal concentration decreased in layer 10 before increasing again at the top of the zone.

304 Zone IP5 (layers 4-1; 2800-1000 cal yr BP) had elevated levels of *Pinus* (36-46%), and
305 *Picea* values that were comparable to Zone IP4 (4-7%). *Artemisia* levels were moderate (19%),
306 and Poaceae levels dropped to the lowest of the record (7-13%). Asteroideae, Rosaceae, and
307 Fabaceae levels increased (5-8%, 4-6%, and 1-7% respectively), as did those of other shrubs and
308 herbs, such as *Eriogonum*. AP:NAP increased in this zone to the second highest level of the
309 record (highest at the very base of the core), and microscopic charcoal increased as well. *Picea*,
310 *Pinus*, and *Abies* needle fragments, Poaceae parts (stems, leaves, florets, and caryopses),
311 *Polygonum* sp., *Plagiobothrys* sp., and Caryophyllaceae seeds, and *Juniperus* sp. leaves were all
312 present in this zone.

313 Surface organic matter on TL1 had high amounts of *Pinus* pollen (58%) and *Picea* pollen
314 (8%). *Artemisia* levels were slightly less than in the deeper samples (10%), and Poaceae
315 increased from Zone IP5 but was lower than in previous zones (14%). AP:NAP increased from
316 Zone IP5, and charcoal decreased slightly.

317

318 [Insert Figure 2]

319

320 ***Meltwater Pond***

321

322 *Lithology*

323 Meltwater Pond sediment cores totaled 93 cm in length. The top 13 cm consisted of dark
324 brown watery peat, which transitioned to dark brown large detritus peat from 20-36 cm depth. At
325 36 cm depth, there was a transition to medium-brown fine detritus gyttja until 60 cm depth. At
326 60 cm depth, there was a lithological change from gyttja to medium-brown-to-gray clay, which
327 persisted to the bottom of the core (Fig. 3).

328

329 [Insert Figure 3]

330

331 *Chronology*

332 The Meltwater Pond age-depth model was based on six AMS radiocarbon ages (Table 2;
 333 Fig. 4). The change in sediment deposition rate and lithology at 60 cm depth suggests a hiatus
 334 from ca. 4200-3000 cal yr BP.

335

336 **Table 2.** Meltwater Pond radiocarbon information.

Core	Depth (cm)	Lab Number/Reference	Material Dated	Uncalibrated Age (¹⁴ C yr BP)	Calibrated Age Range (Cal yr BP) (Probability)
MP1	30	155578	Bulk sediment	405 ± 20	448-508 (.93)
MP1	45	175596	Bulk sediment	1790 ± 20	1621-1670 (.62)
MP1	57	175597	Bulk sediment	2760 ± 20	2780-2884 (.92)
MP1	61	155579	Bulk sediment	4010 ± 25	4418-4524 (1.0)
MP1	80	175598	Bulk sediment	5540 ± 25	6291-6357 (.65)
MP1	95	155580	Bulk sediment	5060 ± 25	5741-5900 (1.0)

337

338 [Insert Figure 4]

339

340 *Pollen and charcoal*

341 The Meltwater Pond pollen record was divided into four zones based on a constrained
 342 cluster analysis (Grimm, 1987). *Pinus*, *Picea* *Artemisia*, Poaceae, Asteroideae, and Cyperaceae
 343 dominated most pollen spectra (Fig. 5).

344 Zone MP1 (100-75 cm depth; >6000-5100 cal yr BP,) had high amounts of *Pinus* (37%-
 345 47%) and *Picea* (7-8%), and moderate amounts of shrubs, herbs, and grasses including *Artemisia*
 346 (13-20%), Poaceae (16-24%), and Asteroideae (3-7%). This assemblage is consistent with an
 347 open *Pinus/Picea Artemisia/Poaceae* parkland. AP:NAP was higher than average during this
 348 zone, suggesting a period when subalpine forests were dense. There was a fire episode at the
 349 base of the core, therefore CHAR and BCHAR were high (relative to the rest of the core) at the
 350 base and decreased towards the top of the zone (0.28-.04 and 0.14-.04 grains/cm²/yr,
 351 respectively).

352 Zone MP2 (75-52 cm depth; ca. 5100-2300 cal yr BP) pollen data were similar to Zone
 353 MP1 representing subalpine parkland, with high amounts of *Pinus* (42-47%), and slightly higher
 354 amounts of *Picea* (6-10%), which declined throughout the zone. Poaceae and *Artemisia*
 355 decreased slightly (12-22%; 12-17%, respectively), and Asteroideae increased (5-9%).

356 Cyperaceae values increased from the base to the top of the zone (0.4-9%). AP:NAP was above
357 average at the base of the zone and then declined. Two small fire episodes were identified, but
358 CHAR and BCHAR remained low throughout the zone (<0.06 and <0.05 grains/cm²/yr,
359 respectively).

360 Zone MP3 (52-36 cm depth; ca. 2300-990 cal yr BP) had the highest abundance of
361 grasses and the lowest amount of arboreal pollen. *Pinus* levels decreased (50-23%), and Poaceae
362 levels increased to the highest of the record (27-48%). Pollen percentages of *Picea*, *Artemisia*,
363 and Asteroideae also decreased (5-2%, 16-10%, and 7-0%, respectively). These data suggest
364 expanded grassland at the expense of forest. CHAR and BCHAR increased from the previous
365 zone (0.01-0.09 grains/cm²/yr), but were still minimal, with two fire episodes during this period.

366 Zone MP4 (36-7 cm depth; ca. 990 cal yr BP-present day) had the highest amounts of
367 *Pinus* pollen of the record (28-59%), which generally increased through the zone with the
368 exception of a decrease from 22-9 cm (ca. 350-150 cal yr BP). *Artemisia* increased in this zone
369 (9-24%), Poaceae decreased (34-18%), and Cyperaceae abundance increased until the top three
370 samples when it dropped (3-17%). AP:NAP increased through the zone (other than with the
371 decrease in *Pinus* at ca. 350-150 cal yr BP), suggesting an increase in the density of subalpine
372 forests through the late Holocene. The surface sample AP:NAP (-0.02) is slightly higher than the
373 long-term average (-0.05). Fluctuations from the long-term average likely represent increases
374 and decreases in subalpine forest density compared to present day. CHAR and BCHAR
375 increased in this zone (.01-0.6 and 0.01-0.24 grains/cm²/yr, respectively), and one fire episode
376 was recorded. The CHAR record only goes until 300 cal yr BP, and the most recent fire episode
377 occurred at ca. 344 cal yr BP.

378

379 [Insert Figure 5]

380

381 **Discussion**

382

383 ***Paleoenvironmental reconstructions from the TL1 Ice Patch and Meltwater Pond***

384

385 Paleoenvironmental records derived from organic layers preserved within an
386 approximately 10,400-year-old ice patch and a 6200-year-old wetland provide new information

387 on past environmental conditions on the Beartooth Plateau. These records highlight dynamic
388 shifts in forest position and changes in the alpine environment in response to climate variations
389 throughout the Holocene. Here, we compare the TL1 Ice Patch and Meltwater Pond sediment
390 records with other regional proxy records to gain a broader picture of past environmental change
391 in the Greater Yellowstone Ecosystem and northern Rocky Mountains. We discuss the
392 conditions that led to the formation of organic layers, and how the information contained within
393 them underscores the potential for ice patches to provide novel records of past climate and
394 environmental change at high elevations.

395

396 ***Late-glacial to early Holocene transition (>10,200 cal yr BP): Ice patch formation and***
397 ***subalpine parkland development***

398

399 Deglaciation of the Beartooth Plateau occurred in the region between ca. 16,000 and
400 13,000 cal yr BP (Licciardi and Pierce, 2018). A moraine at Emerald Lake (2790 m asl; Fig. 1)
401 has been dated to ~12,500 cal yr BP, which suggests that high-elevation glaciers (possibly a
402 resurgence during the Younger Dryas) still persisted on the Beartooth Plateau in the vicinity of
403 the study site at that time (Barth et al., 2022). Although there was late Pleistocene ice in the TL1
404 location during the Last Glacial Maximum, lack of evidence for ice deformation or movement in
405 the cores suggests the TL1 was not a remnant of a larger glacier (Chellman et al., 2021). The age
406 of the oldest organic layer in the TL1 core suggests ice-patch formation at ca. 10,400 cal yr BP,
407 several centuries after glacial retreat.

408 Pollen and macrofossil evidence from the oldest organic layer dating to ca. 10,400 cal yr
409 BP suggests that TL1 formed during a time when the area supported parkland with *Pinus* and
410 *Picea* (Fig. 2). Pollen data from nearby Beauty Lake (Spaulding et al., 2020) and Rainbow Lake
411 (Rust and Minckley, 2020) indicate tundra vegetation was the dominant cover type before the
412 formation of the TL1, depicting a cold, dry, and newly exposed postglacial environment. These
413 records then track the development of *Pinus* and *Picea* parkland at higher elevations, at 2874 m
414 (Beauty Lake) at ca. 11,500 cal yr BP, and then at 2963 m (Rainbow Lake) at ca. 11,000 cal yr
415 BP. Conifers migrated upslope during the late-glacial to early-Holocene transition, in response to
416 warmer and possibly wetter climatic conditions after the Last Glacial Maximum (Alder and
417 Hostetler, 2015; Bartlein et al., 1998; Krause and Whitlock, 2017).

418 Lake-level reconstructions in the region indicate a dry, late-glacial period and an increase
419 in moisture into the early Holocene (Shuman et al., 2010; Shuman and Serravezza, 2017).
420 Rainbow Lake and Lake of the Woods, WY (150 km to the south) both deepened at ca. 11,300
421 cal yr BP (Shuman et al., 2010; Shuman and Serravezza, 2017). This is likely the result of
422 increased moisture brought to the region by changes in mid-continent atmospheric circulation,
423 such as the northerly shift of the westerly mid-latitude jet stream in response to the retreating
424 Laurentide ice sheet (Alder and Hostetler, 2015; Bartlein et al., 1998). Other sites at lower
425 elevations in the GYE also recorded effectively wetter summers during the early Holocene,
426 implying increased winter snowpack or increased convection summer storms (Krause and
427 Whitlock, 2013). Many pollen records in the GYE indicate an increase in forest density at this
428 time as well (Benes et al., 2019; Iglesias et al., 2018; Krause et al., 2015; Whitlock, 1993;
429 Whitlock et al., 2012). Increasing moisture in addition to warming summer temperatures after the
430 late-glacial period allowed infilling of forests and an upslope expansion of conifers to higher
431 elevations.

432 The formation of TL1 during early-Holocene warming is likely a result of the increased
433 precipitation in the region and/or cooler winter temperatures. TL1 $\delta^{18}\text{O}$ evidence indicates this
434 time was a period of relatively cooler winter temperatures and/or enhanced snowfall (Chellman
435 et al., 2021). During the early Holocene, paleoclimate model simulations (Alder and Hostetler,
436 2015; Bartlein et al., 1998) suggest that increasing summer insolation and decreasing winter
437 insolation (Berger, 1978) brought about warmer summers and cooler winters than today in this
438 region. Ice accumulation could have increased with the development of permafrost on exposed
439 ground during the cooler winters.

440

441 ***Early Holocene (~10,200-6200 cal yr BP): Steppe formation***

442

443 By 9000 cal yr BP, the high-elevation *Pinus* and *Picea* parkland was replaced by steppe
444 vegetation, which persisted for approximately 3000 years. This shift is indicated by the decrease
445 in *Pinus* pollen and increase in *Artemisia* and Poaceae pollen in the TL1 organic layers (Fig. 2).
446 Low elevation sites in the GYE also record an expansion of steppe and xerophytic conifers from
447 ca. 10,200-7500 cal yr BP (Iglesias et al., 2018; Krause and Whitlock, 2013; Krause et al., 2015;
448 Schiller et al., 2022; Whitlock, 1993; Whitlock et al., 2012), suggesting regional warm and dry

449 conditions. The Rainbow Lake record showed little change in vegetation after the initial increase
450 of *Pinus* at 11,000 cal yr BP (Rust and Minckley, 2020), and the pollen record from Beauty Lake
451 indicates only a small increase in Poaceae and *Artemisia* at 10,000 cal yr BP (Spaulding et al.,
452 2020). These lakes are located at elevations currently below modern treeline. Therefore, it is
453 possible parklands persisted near those sites, or due to their larger size, they recorded a more
454 regional signal from forests at lower elevations.

455 Although a lowering of treeline could signify cooler conditions (Harsch and Bader, 2011;
456 Morgan et al., 2014), higher summer insolation levels (Berger, 1978) and paleoclimate model
457 simulations suggest this region experienced greater summer drought in the early Holocene than
458 at present due to an expansion of the Pacific high-pressure system (Alder and Hostetler, 2015;
459 Bartlein et al, 1998; Thompson et al., 1997). Conifer tree establishment is often temperature
460 dependent but moisture limitation impacts tree success as well, so the continued summer
461 warming during the early Holocene could have decreased effective moisture and prevented tree
462 growth. Significant shallowing of Rainbow Lake (Fig. 6) is consistent with hot summers leading
463 to greater evaporative demand (Shuman and Serravezza, 2017), and MP had not yet formed,
464 likely because summers were too dry. The TL1 $\delta^{18}\text{O}$ record shows colder-than-present winter
465 temperatures throughout this period (Chellman et al., 2021; Fig. 6), though this may be evidence
466 of strong seasonality and does not preclude warm dry summers. Severe winter temperatures
467 could have additionally caused tree damage and dieback on the Beartooth Plateau.

468

469 [Insert Figure 6]

470

471 ***Middle Holocene (6200-4200 cal yr BP): Parkland development***

472

473 Drought conditions lessened after ca. 6200 cal yr BP, as evidenced by the initiation of
474 sediment accumulation in MP, as well as increased levels of conifer pollen in both the TL1 and
475 MP records (Figs. 2 and 5). MP sediment accumulation suggests effective precipitation increased
476 (or warm season evapotranspiration decreased) enough to allow surplus runoff to collect in the
477 topographic depression. The increase in effective moisture supported an upslope shift in treeline.
478 Both records suggest the presence of *Pinus* and *Picea* parkland with areas of tundra dominated
479 by *Artemisia* and Poaceae.

480 The onset of wetter conditions at ca. 6000 cal yr BP is also evident in other records of the
481 GYE and northern Rocky Mountains. Many lake pollen records show an increase in forest
482 density at ca. 6000-5000 cal yr BP (Alt et al., 2018; Brunelle et al., 2005; Mack et al., 1978;
483 McWethy et al., 2020; Mehringer et al., 1977). In addition to the formation of the MP, other
484 lakes in Montana and Wyoming (including Rainbow Lake) deepened around ca. 5500 cal yr BP
485 (Minckley et al., 2012; Shuman and Serravezza, 2017), and the synchronous increase of TL1
486 $\delta^{18}\text{O}$ values suggests that winters warmed during this period (Fig. 6; Chellman et al., 2021). The
487 enhanced seasonality of the early Holocene lessened as orbital changes caused a progression
488 toward modern seasonal insolation levels. This potentially resulted in an increase in winter
489 precipitation and a decrease in summer evaporative demand, enabling conifer expansion and lake
490 level rise (Marsicek et al., 2018; Shuman et al., 2009; Whitlock et al., 2012).

491 The MP record suggests the presence of trees at higher elevations until ca. 4500 cal yr BP
492 when arboreal pollen decreased until ca. 4200 cal yr BP (Fig. 6). Arboreal pollen in the TL1
493 record declined at ca. 5000 cal yr BP, although macrofossil evidence suggests that *Picea* was still
494 locally present (Figs. 2 and 6). Although the TL1 arboreal pollen rose slightly after 5000 cal yr
495 BP, the downward trend from ca. 6000 cal yr BP to ca. 4200 cal yr BP in both records suggests
496 that treeline once again shifted downslope. With no evidence for a decrease in regional moisture,
497 the downslope shift in treeline elevation at this time was likely in response to cooling
498 temperatures.

499

500 ***Late Holocene (4200 cal yr BP-present day): Shifts between parkland and steppe***

501

502 After ca. 4200 cal yr BP, there is evidence for another shift in the environment and
503 climate of the Beartooth Plateau. The MP age-depth model suggests extremely slow deposition
504 and/or a hiatus between ca. 4200-3000 cal yr BP (Fig. 4), and a lithological change from fine
505 detritus/clay at ca. 4200 cal yr BP to more organic-rich sediment by ca. 2900 cal yr BP within 3
506 cm of the core supports a hiatus occurred (Fig. 3). Hiatuses are commonly caused by drought,
507 although the pollen in the sample immediately below the hiatus shows no evidence of
508 degradation to suggest post-deposition subaerial exposure. We suggest that the hiatus resulted
509 from colder conditions that covered MP with snow and/or ice for a long portion of the year, with
510 the extended ice cover preserving the pollen but preventing sediment accumulation. The pollen

511 accumulation rate in the sample below the hiatus was extremely high, supporting this scenario of
512 pollen influx despite little sediment accumulation – which would be unlikely in a desiccated
513 pond. The sample below the hiatus additionally shows a decrease in forest density, indicating
514 treeline decline coincided with increased snow accumulation and colder temperatures. At TL1,
515 the decrease of *Pinus* at ca. 3200 cal yr BP and increase in *Artemisia* and Poaceae at the end of
516 the hiatus are also consistent with lowering of treeline elevation and colder summer conditions
517 (Fig. 2 and 6).

518 Evidence from other sites also suggests that cool and relatively wet conditions prevailed
519 during this hiatus interval. Beginning around ca. 3900 cal yr BP, the TL1 $\delta^{18}\text{O}$ record declined
520 and ice accretion rates more than doubled likely indicating cool, wet winters and cool summers
521 (Fig 6; Chellman et al., 2021). Similarly, at ca. 6300 cal yr BP, the Teton Glacier in the Teton
522 Range, WY (~160 km to the southwest of the Beartooth Plateau) advanced slowly (coinciding
523 with the decrease in summer temperatures and increase in effective moisture seen in the TL1
524 record), and then advanced dramatically between 3900-2800 cal yr BP, after which it retreated
525 (Larsen et al., 2020). Fairy Lake, a high-elevation site in the northern part of the GYE, recorded
526 an increase in snow avalanches at ca. 4500-2000 cal yr BP, signifying higher snowpack and
527 unstable late-season snow conditions (Benes et al., 2019). Other mid-elevation forests in the
528 northern Rocky Mountains region also experienced an increase in mesophytic trees such as *Picea*
529 and *Abies* during this time period, which may have been in response to increases in moisture and
530 cool conditions (Alt et al., 2018; Mack et al., 1978, 1978, 1983; Mehringer et al., 1985;
531 McWethy et al., 2020). The Rainbow Lake record, while rather stable after the dramatic rise at
532 ca. 5900 cal yr BP, indicates a slight additional deepening at ca. 4100 cal yr BP (Fig. 6; Shuman
533 and Serravezza, 2017). Although the timing is asynchronous among records, it is probable that
534 the Beartooth Plateau and other nearby mountainous regions experienced the coldest wettest
535 conditions of the postglacial period from ca. 4000-3000 cal yr BP.

536 Although evidence supports a cold and wet period, other regional records indicate the
537 possibility of drought conditions during the MP hiatus. The timing of the hiatus is not definitive
538 (after ca. 4400 until before ca. 2900 cal yr BP based on the two surrounding radiocarbon dates),
539 but 4200-3800 cal yr BP corresponds to a period in the TL1 $\delta^{18}\text{O}$ record that suggests warm dry
540 winter conditions (Chellman et al., 2021). Diatom records from lakes on the Beartooth Plateau
541 (Emerald Lake and Beauty Lake) similarly suggest the lake thermal structures from ca. 4500-

542 3200 cal yr BP were similar to today, and cold harsh winters (represented by deeper lake
543 mixing), did not exist until one thousand years later at ca. 3200-2300 cal yr BP (Stone et al.,
544 2016). Therefore, it is possible the MP hiatus was the result of desiccation during a warm dry
545 period that also affected the plains and the midcontinent (Diffenbaugh et al., 2006; Liefert and
546 Shuman, 2020, 2022). Yellowstone Lake and Lake of the Woods, WY additionally had low
547 water periods until ca. 3000 cal yr BP (Pierce et al., 2002; Shuman et al., 2010). However, the
548 presence of abundant pollen with few signs of degradation (i.e., from exposure) in the MP core,
549 and the possibility that the difference in timing could be the result of age-depth uncertainty
550 suggests the MP drying scenario is less plausible.

551 Following this cool, wet period, there is evidence that trees returned to higher elevations
552 between ca. 3000-2000 cal yr BP. Both TL1 and MP records show high amounts of *Pinus* and
553 moderate levels of Poaceae and *Artemisia*, suggesting an open parkland (Figs. 2 and 5). The
554 Rainbow Lake record features a slight increase in *Pinus* during this period (Rust and Minckley,
555 2020; Fig. 7), and many records in the northern Rocky Mountains indicate the establishment of
556 modern forest composition after ca. 3000 cal yr BP (Alt et al., 2018; McWethy et al., 2020;
557 Whitlock et al., 2012). Though this suggests relatively stable climate conditions during recent
558 millennia, the MP record indicates more variability in forest dynamics at high elevations on the
559 Beartooth Plateau.

560 At ca. 2000 cal yr BP, Poaceae pollen increases in the MP record and reaches a maximum
561 at ca. 1000 cal yr BP. This increase marks a transition to alpine tundra and a downslope shift in
562 treeline (Figs. 5 and 7). In contrast, the TL1 record has moderate amounts of Poaceae pollen and
563 *Pinus* and *Picea* percentages equivalent to those at the base of the record at ca. 10,400 cal yr BP,
564 which are interpreted as parkland. The abundance of Poaceae macrofossils declined at 2000 cal
565 yr BP (SM Fig. 2), and leaf and stem macrofossils (SM Fig. 2) and Asteroideae and Rosaceae
566 pollen increased (Fig. 2). Thus, the TL1 record suggests an open landscape with shrubs and
567 possibly scattered trees. The TL1 record ends with a similar, although less sharp, downward
568 trend in the AP:NAP ratio, also implying a transition towards open conditions (Fig. 6).

569 Few other records in the region suggest a change in vegetation at ca. 2000 cal yr BP
570 similar to those recorded in the Beartooth sites but several records show evidence of drought at
571 this time. For example, diatom data from low-elevation Crevice Lake in the GYE, register
572 shortened springs and longer summers (Whitlock et al., 2012), and charcoal data at several sites

573 in the northern Rocky Mountains indicate increased fires at ca. 2000 cal yr BP, possibly
574 signifying warm and dry conditions (Alt et al., 2018; Brunelle et al., 2005). A 2000-year-long
575 streamflow reconstruction for the Upper Colorado River, to the south of the Beartooth Plateau,
576 indicates a severe 2nd century drought unmatched in terms of magnitude and duration
577 (Gangopadhyay et al., 2022). While the grassland period seen in the MP record precedes the
578 Medieval Climate Anomaly (MCA), the decrease in treeline indicates either the onset of drier
579 conditions leading into the MCA or intensified cooling (Shuman and Marsicek, 2016).

580 Our records indicate that vegetation on the Beartooth Plateau responded to both the MCA
581 (1000-750 cal yr BP; Cook et al., 2004) and the Little Ice Age (LIA; 500-250 cal yr BP; Cook et
582 al., 2010; Mann et al., 1999). The TL1 record ends during the MCA with evidence of *Pinus*
583 presence, and the MP record displays an increase in arboreal pollen throughout the MCA. Other
584 GYE high-elevation sites also show denser forests at ca. 1500 cal yr BP (Iglesias et al., 2018),
585 and stumps above present-day treeline that date to between 1500-800 cal yr BP in central
586 Yellowstone National Park (Meyer et al., 1995) and in the Wind Rivers Range, WY (Morgan et
587 al., 2014) suggest that trees migrated upslope during the prolonged warm conditions of the
588 MCA.

589 Following the MCA, MP *Pinus* and *Picea* pollen decreased between ca. 500-300 cal yr
590 BP, coincident with the LIA. *Artemesia* expanded around Beauty Lake (Spaulding et al., 2020),
591 and other high-elevation sites in the GYE recorded a decrease in conifer pollen (Iglesias et al.,
592 2018). This suggests that high-elevation trees shifted downslope in response to the colder
593 conditions of the LIA. After the LIA cooling, arboreal pollen in the MP record increased to
594 present day, which reflects the treeline migration upslope to its current position in response to
595 warming conditions.

596

597 [Insert Figure 7]

598

599 ***Holocene fire history***

600

601 During the early Holocene, TL1 microcharcoal concentrations started high, but decreased
602 between ca. 9500-6000 cal yr BP, paralleling the decrease in conifer tree pollen (Figs 5 and 6).
603 Both the TL1 and MP records show elevated charcoal accumulation at ca. 6000 cal yr BP when

604 there is evidence of a return of trees to higher elevations. Charcoal in the MP record decreased
605 after ca. 5700 cal yr BP, while TL1 charcoal concentrations remained high until ca. 4000 cal yr
606 BP. Since the TL1 charcoal is microscopic and that at MP is macroscopic, this difference could
607 be explained by grass fires or long-distance transport of microscopic charcoal versus the local
608 forest and shrub fires registered in the macroscopic (predominantly woody) charcoal records
609 (Leys et al., 2017). The records from Rainbow and Beauty Lakes also showed minimal charcoal
610 throughout their records, although an increase in fire activity at ca. 6000-5500 cal yr BP (Rust
611 and Minckley, 2020; Spaulding et al., 2020) supports an increase in fire activity on the Beartooth
612 Plateau consistent with the pollen interpretation of forest expansion during this time period.

613 The TL1 charcoal declined during the period when the MP record shows a hiatus. If the
614 hiatus was in response to drought, we would expect more evidence of fire in the TL1 record, so
615 the lack of charcoal supports our hypothesis that the hiatus was due to cold temperatures and
616 greater ice cover. The MP record in the late Holocene shows one more increase in charcoal after
617 ca. 1000 cal yr BP, again paralleling an increase in conifer pollen, suggesting fire activity
618 returned to high elevations when there was fuel to burn.

619

620 *Organic layers from ice patches as a novel paleoenvironmental proxy*

621

622 Our analysis of pollen, charcoal, and macrofossils from organic layers deposited in ice
623 cores is the first record of this type for North America. Previous efforts to analyze pollen from
624 sediment within perennial ice deposits in high-elevation caves in the Pyrenees succeeded in
625 creating a record of altitudinal treeline fluctuation over the mid-to-late Holocene (Leunda et al.,
626 2019). While the Pyrenees ice cave deposits are formed through processes that are different than
627 those that result in the development of high-elevation ice patches, the organic layers in both ice
628 deposits are thought to be related to acute periods of ablation (Leunda et al., 2019; Chellman et
629 al., 2021). Chellman et al. (2021) propose that the organic layers in the ice patch formed as
630 windblown or animal-deposited material collected on the summer snowpack, which then
631 concentrated into one organic-rich layer during periods of surface melt and ablation. The most
632 recent TL1 organic layer dates to ca. 1000 cal yr BP, which corresponds to the MCA, supporting
633 the hypothesis that the organic layers form during periods of warm and possibly dry conditions
634 (Chellman et al., 2021).

635 In contrast with continuous wetland records, the ice patch organic layers record
636 represents discontinuous snapshots in time. If the layers represent severe, multi-decadal drought
637 events, their duration is likely within the range of multi-decadal droughts documented in tree-
638 ring records from the western US (Ault et al., 2013, 2018; Cook et al., 2010). The absence of
639 major discontinuities in the TL1 ice accumulation chronology suggests the droughts were not
640 sufficiently long or intense enough to melt the ice patch enough to result in significant mass loss
641 or chronological discontinuities. Droughts severe enough to generate an organic layer occurred
642 on average every few hundred years throughout the Holocene, which matches the approximate
643 frequency of megadroughts deduced from fire-related sediment runoff in Yellowstone National
644 Park (Meyer et al., 1995) and recorded in tree-ring records over the last millennium (Ault et al
645 2013).

646 Another depositional feature of the ice patch record that is not well understood is the
647 amount and volume of organic sediment deposited in an organic layer. The magnitude of
648 deposition could be related to the duration or severity of a drought, or to the duration of animal
649 activity depositing feces and vegetative matter. It also could be related to periods when strong
650 winds transported and deposited large amounts of organic material onto the ice. If the latter,
651 mass and volume of the organic layers could potentially be used as another paleoclimate proxy.
652 The mass of organic material did increase during times when conifers were more abundant at
653 higher elevations (Table 2; the most recent layers over the past ~2500 years, one at ca. 5800 cal
654 yr BP, and at the very base of the ice core from ca. 10,400-9800 cal yr BP). Thus, increased
655 deposition and preservation of organic material in the ice occurred when subalpine parklands or
656 forests were located at higher elevations. This association suggests that the thicker layers were
657 formed when decadal-scale droughts and anomalous summer warmth resulted in periods of
658 negative mass balance during an overall wetter and cooler time conducive to high-elevation tree
659 growth.

660 Counter to this general pattern, one heavy organic layer formed when treeline elevations
661 were lower (ca. 7800 cal yr BP) during the early Holocene period. This layer contained increased
662 levels of animal digesta and may have formed during a time of high animal occupation of the ice
663 patch, possibly as a water source during summer drought. The longest consecutive sequence of
664 light organic layer masses (<1g) occurred between ca. 5100-2800 cal yr BP, which is a period of
665 increased ice accumulation and cooler summers with more effective cool-season precipitation

666 (Fig 6). This time may have been characterized by shorter and less severe droughts as well as
667 less intense use of ice patches by ungulates.

668

669 **Conclusions**

670

671 The Beartooth TL1 Ice Patch and Meltwater Pond records provide new insight into high-
672 elevation treeline dynamics and climate change during the Holocene. During the late-glacial to
673 early Holocene transition, treeline elevation rose with warmer temperatures and increased
674 moisture (Fig. 7). As summer insolation levels continued to increase and winter insolation levels
675 decreased after ca. 10,000 cal yr BP, cold harsh winters and dry summers led to increased tree
676 mortality and a lowering of treeline elevation despite warmer growing season temperatures.
677 After ca. 6200 cal yr BP, relatively cooler summers and warmer, wetter winters than before led
678 to the formation of the Meltwater Pond and an increase in Rainbow Lake water levels (Fig 6).
679 Subalpine conifers established at higher elevations, and fire activity increased due to more fuel
680 availability. By 5000 cal yr BP, treeline elevation decreased again, possibly caused by a return of
681 cooler winter and summer conditions. An increase in ice accumulation and an apparent hiatus in
682 the MP core suggests the high-elevation basin had more perennial snow and ice coverage during
683 a possible neoglacial period spanning from ca. 4000 to 3000 cal yr BP (Fig. 6 and 7). After the
684 MP hiatus, treeline rose in elevation from ca. 3000 to ca. 2000 cal yr BP, in response to warming
685 temperatures after the neoglacial period and then decreased until the onset of the MCA, perhaps
686 in response to persistent drought or cooler summer temperatures. Treeline advanced in response
687 to warming conditions during the MCA, lowered with cold summer temperatures during the LIA,
688 and then gradually rose to its present location.

689 Although climate projections suggest that temperatures will rise 4 to 6°F higher in the
690 coming decades (Hostetler et al. 2021), this warming may not lead to an expansion of forest
691 cover on the Beartooth Plateau. The paleoecological evidence from TL1 and MP show a
692 nonlinear response to warming temperatures in the past. Conifer forests on the Beartooth Plateau
693 declined during a time of increased summer drought in the early Holocene despite warmer
694 temperatures. During the late Holocene, relatively warmer winters and cooler summers were the
695 primary limitations of treeline elevation, allowing treeline to move upslope. Recent and projected
696 climate conditions suggest a shift in the seasonality of precipitation will reduce growing season

697 moisture availability (Hostetler et al. 2021), and it is likely that high-elevation forests will again
698 become moisture limited, decreasing density and ultimately lowering treeline as occurred during
699 the early Holocene.

700 While the exact processes behind the deposition and preservation of organic material in
701 the ice patch are uncertain, it is likely that they occur during extended periods of drought. It is
702 possible that these organic layers represent landscape vegetation during a drought spanning
703 multiple decades but the continuity of ice accumulation precludes the droughts from lasting
704 much longer. Therefore, even though one TL1 organic layer sample could represent decades, the
705 layers are thought to be capturing snapshots of more gradual long-term vegetation changes, and
706 not a decades-long vegetation change within the timespan of the drought period. If our
707 understanding of the organic layer formation and accretion of material in the ice is accurate, the
708 TL1 record suggests that extended and severe droughts were common throughout the Holocene,
709 occurring at least 29 times over the last 10,400 years – or on average once every ~300 years.

710 Although questions remain about the formation and persistence of ice patches and the
711 layers within, recent investigations show that they can serve as a paleoenvironmental record,
712 providing new climate and ecosystem insights that complement information derived from
713 traditional paleoenvironmental records. In order to better interpret these records, future research
714 could seek to better understand the specific processes and mechanisms that underly their
715 formation. Additionally, the human artifacts and biological information frozen within ice patches
716 (pollen, macrofossils, etc.) combined with their physical record of ice accumulation rates, water
717 isotopes, as well as frequency and timing of organic layer development make them unique
718 recorders of the combined human-climate-ecosystem response. Paleoenvironmental records from
719 ice patches present a unique opportunity to generate a greater understanding of the effects of
720 seasonal climate changes on high-elevation ecosystems, and the organic layers can augment
721 traditional analyses of proxies from wetland sediments by highlighting extreme climatic events
722 as well as documenting the more gradual ecological change in areas with few
723 paleoenvironmental proxies.

724

725

726

727

728 **Declaration of competing interest**

729

730 The authors declare that they have no known competing financial interests or personal
731 relationships that could have appeared to influence the work reported in this paper.

732

733 **Acknowledgments**

734

735 We thank U. Wisconsin Ice Drilling Design and Operations, M. Jayred for assistance in drilling
736 the ice cores and all of the project field and laboratory assistants. Any use of trade, firm, or
737 product names is for descriptive purposes only and does not imply endorsement by the U.S.
738 Government.

739

740 **Funding**

741

742 The author(s) disclosed receipt of the following financial support for the research, authorship,
743 and/or publication of this article: This project was funded by the NSF [grant BCS 1832486] as
744 well as the Buffalo Bill Historical Center's Draper Natural History Museum, University of
745 Wyoming's Biodiversity Institute, Prince Albert II of Monaco Foundation—Monaco and USA,
746 the U.S. Geological Survey Ecosystem Program and Climate Research and Development
747 Program, INSTAAR, and the Sulo and Aileen Maki Endowment at the Desert Research Institute.

748

749 **References**

750

751 Alder JR and Hostetler SW (2015) Global climate simulations at 3000-year intervals for the last
752 21 000 years with the GENMOM coupled atmosphere–ocean model. *Climate of the Past*
753 11(3). Copernicus GmbH: 449–471. DOI: 10.5194/cp-11-449-2015.

754 Alt M, McWethy D, Everett R, et al. (2018) Millennial scale climate–fire–vegetation interactions
755 in a mid-elevation mixed coniferous forest, Mission Range, northwestern Montana, USA.
756 *Quaternary Research* 90: 1–17. DOI: 10.1017/qua.2018.25.

757 Andrus RA, Harvey BJ, Rodman KC, et al. (2018) Moisture availability limits subalpine tree
758 establishment. *Ecology* 99(3): 567–575. DOI: 10.1002/ecy.2134.

759 Ault TR, Cole JE, Overpeck JT, et al. (2013) The Continuum of Hydroclimate Variability in
760 Western North America during the Last Millennium. *Journal of Climate* 26(16): 5863–
761 5878. DOI: 10.1175/JCLI-D-11-00732.1.

762 Ault TR, St. George S, Smerdon JE, et al. (2018) A Robust Null Hypothesis for the Potential
763 Causes of Megadrought in Western North America. *Journal of Climate* 31(1): 3–24. DOI:
764 10.1175/JCLI-D-17-0154.1.

765 Barth AM, Ceperley EG, Vavrus C, et al. (2022) ¹⁰Be age control of glaciation in the Beartooth
766 Mountains, USA from the latest Pleistocene through the Holocene. *Geochronology
767 Discussions*. Copernicus GmbH: 1–18. DOI: 10.5194/gchron-2022-17.

768 Bartlein PJ, Anderson KH, Anderson PM, et al. (1998) Paleoclimate simulations for North
769 America over the past 21,000 years: features of the simulated climate and comparisons
770 with paleoenvironmental data. *Quaternary Science Reviews* 17(6): 549–585. DOI:
771 10.1016/S0277-3791(98)00012-2.

772 Benedict JB (2011) Sclerotia as indicators of mid-Holocene tree-limit altitude, Colorado Front
773 Range, USA. *The Holocene* 21(6): 1021–1023. DOI: 10.1177/0959683610395078.

774 Benedict JB, Benedict RJ, Lee CM, et al. (2008) Spruce trees from a melting ice patch: evidence
775 for Holocene climatic change in the Colorado Rocky Mountains, USA. *The Holocene*
776 18(7). SAGE Publications Ltd: 1067–1076. DOI: 10.1177/0959683608095578.

777 Benes J, Iglesias V and Whitlock C (2019) Postglacial vegetation dynamics at high elevation
778 from Fairy Lake in the northern Greater Yellowstone Ecosystem, Montana, USA.
779 *Quaternary Research* 92: 1–16. DOI: 10.1017/qua.2019.9.

780 Bennett KD and Willis KJ (2001) Pollen. In: Smol JP, Birks HJB and Last WM (eds) *Tracking
781 Environmental Change Using Lake Sediments: Terrestrial, Algal, and Siliceous
782 Indicators*, 3. Dordrecht: Kluwer Academic Publishers, pp. 5–32.

783 Berger A (1978) Long-term variations of caloric insolation resulting from the earth's orbital
784 elements. *Quaternary Research* 9: 139–167.

785 Blaauw M and Christen JA (2011) Flexible paleoclimate age-depth models using an
786 autoregressive gamma process. *Bayesian Analysis* 6(3). International Society for
787 Bayesian Analysis: 457–474. DOI: 10.1214/11-BA618.

788 Brunelle A, Whitlock C, Bartlein P, et al. (2005) Holocene fire and vegetation along
789 environmental gradients in the Northern Rocky Mountains. *Quaternary Science Reviews*
790 24(20–21): 2281–2300. DOI: 10.1016/j.quascirev.2004.11.010.

791 Cappers RTJ and Bekker RM (2013) *A Manual for the Identification of Plant Seeds and Fruits.*
792 Groningen Archaeological Studies, Vol. 23. Eelde: Barkuis Publishing.

793 Carlquist S (1988) *Comparative Wood Anatomy*. Berlin: Springer-Verlag.

794 Chellman NJ, Pederson GT, Lee CM, et al. (2021) High elevation ice patch documents Holocene
795 climate variability in the northern Rocky Mountains. *Quaternary Science Advances* 3:
796 100021. DOI: 10.1016/j.qsa.2020.100021.

797 Cook ER, Woodhouse CA, Eakin MC, et al. (2004) Long-term aridity changes in the western
798 United States. *Science* 306: 1015–1018.

799 Cook ER, Seager R, Heim RR, et al. (2010) Megadroughts in North America: placing IPCC
800 projections of hydroclimatic change in a long-term palaeoclimate context: Megadroughts
801 in North America. *Journal of Quaternary Science* 25(1): 48–61. DOI: 10.1002/jqs.1303.

802 Core HA, Côté WA and Day AC (1976) *Wood Structure and Identification*. New York: Syracuse
803 University Press.

804 Delorit RJ (1970) *An Illustrated Taxonomy Manual of Weed Seeds*. River Falls: Wisconsin State
805 University Agronomy Publications.

806 Diffenbaugh NS, Ashfaq M, Shuman B, et al. (2006) Summer aridity in the United States:
807 Response to mid-Holocene changes in insolation and sea surface temperature.
808 *Geophysical Research Letters* 33(22). DOI: <https://doi.org/10.1029/2006GL028012>.

809 Fall PL, Davis PT and Zielinski GA (1995) Late Quaternary Vegetation and Climate of the Wind
810 River Range, Wyoming. *Quaternary Research* 43(3): 393.

811 Faegri K and Iversen J (1989). *Textbook of Pollen Analysis 4th ed.* New Jersey: The Blackburn
812 Press.

813 Gangopadhyay S, Woodhouse CA, McCabe GJ, et al. (2022) Tree Rings Reveal Unmatched 2nd
814 Century Drought in the Colorado River Basin. *Geophysical Research Letters* 49(11):
815 e2022GL098781. DOI: 10.1029/2022GL098781.

816 Grimm EC (1987) CONISS: a FORTRAN 77 program for stratigraphically constrained cluster
817 analysis by the method of incremental sum of squares. *Computers & Geosciences* 13(1):
818 13–35. DOI: 10.1016/0098-3004(87)90022-7.

819 Harsch MA and Bader MY (2011) Treeline form - a potential key to understanding treeline
820 dynamics: The causes of treeline form. *Global Ecology and Biogeography* 20(4): 582–
821 596. DOI: 10.1111/j.1466-8238.2010.00622.x.

822 Heidel B, Fertig W, Mellmann-Brown S, et al. (2017) *Fens and their rare plants in the Beartooth*
823 *Mountains, Shoshone National Forest, Wyoming*. RMRS-GTR-369. Ft. Collins, CO: U.S.
824 Department of Agriculture, Forest Service, Rocky Mountain Research Station. DOI:
825 10.2737/RMRS-GTR-369.

826 Higuera PE, Brubaker LB, Anderson PM, et al. (2009) Vegetation mediated the impacts of
827 postglacial climate change on fire regimes in the south-central Brooks Range, Alaska.
828 *Ecological Monographs* 79(2): 201–219. DOI: 10.1890/07-2019.1.

829 Hoadley RB (1990) *Identifying Wood: Accurate Results with Simple Tools*. Newtown: The
830 Taunton Press.

831 Hoch G and Körner C (2009) Growth and carbon relations of tree line forming conifers at
832 constant vs. variable low temperatures. *Journal of Ecology* 97(1): 57–66. DOI:
833 10.1111/j.1365-2745.2008.01447.x.

834 Hostetler S, Whitlock C, Shuman B, et al. (2021). *Greater Yellowstone climate assessment: past,*
835 *present, and future climate change in greater Yellowstone watersheds*. Bozeman:
836 Montana State University, Institute on Ecosystems. <https://doi.org/10.15788/GYCA2021>.

837 Huerta MA, Whitlock C and Yale J (2009) Holocene vegetation–fire–climate linkages in
838 northern Yellowstone National Park, USA. *Palaeogeography, Palaeoclimatology,*
839 *Palaeoecology* 271(1–2): 170–181. DOI: 10.1016/j.palaeo.2008.10.015.

840 InsideWood (2004). InsideWood Database. Available at: <http://insidewood.lib.ncsu.edu/search>
841 (accessed 2013–2017).

842 Iglesias V, Whitlock C, Krause TR, et al. (2018) Past vegetation dynamics in the Yellowstone
843 region highlight the vulnerability of mountain systems to climate change. *Journal of*
844 *Biogeography* 45(8): 1768–1780. DOI: 10.1111/jbi.13364.

845 Kapp RO, Davis OK and King JE (2000). *Pollen and Spores*. 2nd ed. Dallas: American
846 Association of Stratigraphic Palynologists Foundation.

847 Kelly RF, Higuera PE, Barrett CM, et al. (2011) Short Paper: A signal-to-noise index to quantify
848 the potential for peak detection in sediment–charcoal records. *Quaternary Research*
849 75(1): 11–17. DOI: 10.1016/j.yqres.2010.07.011.

850 Knobel E (1980) *Field Guide to the Grasses, Sedges and Rushes of the United States*. New York:
851 Dover Publications

852 Körner C and Paulsen J (2004) A world-wide study of high altitude treeline temperatures: Study
853 of high altitude treeline temperatures. *Journal of Biogeography* 31(5): 713–732. DOI:
854 10.1111/j.1365-2699.2003.01043.x.

855 Krause TR and Whitlock C (2013) Climate and vegetation change during the late-glacial/early-
856 Holocene transition inferred from multiple proxy records from Blacktail Pond,
857 Yellowstone National Park, USA. *Quaternary Research* 79(3): 391–402. DOI:
858 10.1016/j.yqres.2013.01.005.

859 Krause TR and Whitlock C (2017) Climatic and non-climatic controls shaping early postglacial
860 conifer history in the northern Greater Yellowstone Ecosystem, USA. *Journal of*
861 *Quaternary Science* 32(7): 1022–1036. DOI: 10.1002/jqs.2973.

862 Krause TR, Lu Y, Whitlock C, et al. (2015) Patterns of terrestrial and limnologic development in
863 the northern Greater Yellowstone Ecosystem (USA) during the late-glacial/early-
864 Holocene transition. *Palaeogeography, Palaeoclimatology, Palaeoecology* 422: 46–56.
865 DOI: 10.1016/j.palaeo.2014.12.018.

866 Kyne J and McConnell J (2007) The PrairieDog: a double-barrel coring drill for ‘hand’ augering.
867 *Annals of Glaciology* 47. Cambridge University Press: 99–100. DOI:
868 10.3189/172756407786857703.

869 Larsen DJ, Crump SE and Blumm A (2020) Alpine glacier resilience and Neoglacial fluctuations
870 linked to Holocene snowfall trends in the western United States. *Science Advances* 6(47):
871 eabc7661. DOI: 10.1126/sciadv.abc7661.

872 Lee CM (2012) Withering Snow and Ice in the Mid-latitudes: A New Archaeological and
873 Paleobiological Record for the Rocky Mountain Region. *Arctic* 65. Arctic Institute of
874 North America: 165–177.

875 Lee CM and Puseman K (2017) Ice patch hunting in the Greater Yellowstone area, Rocky
876 Mountains, USA: wood shafts, chipped stone projectile points, and bighorn sheep (*Ovis*
877 *canadensis*). *American Antiquity* 82(2): 223–243. DOI: 10.1017/aaq.2016.32.

878 Lenoir J, Gégout JC, Marquet PA, et al. (2008) A Significant Upward Shift in Plant Species
879 Optimum Elevation During the 20th Century. *Science* 320(5884): 1768–1771. DOI:
880 10.1126/science.1156831.

881 Leunda M, González-Sampériz P, Gil-Romera G, et al. (2019) Ice cave reveals environmental
882 forcing of long-term Pyrenean tree line dynamics. *Journal of Ecology* Leys B (ed.)
883 107(2): 814–828. DOI: 10.1111/1365-2745.13077.

884 Leys BA, Commerford JL and McLauchlan KK (2017) Reconstructing grassland fire history
885 using sedimentary charcoal: Considering count, size and shape. *PLOS ONE* Carcaillet C
886 (ed.) 12(4): e0176445. DOI: 10.1371/journal.pone.0176445.

887 Licciardi JM and Pierce KL (2018) History and dynamics of the Greater Yellowstone Glacial
888 System during the last two glaciations. *Quaternary Science Reviews* 200: 1–33. DOI:
889 10.1016/j.quascirev.2018.08.027.

890 Liefert DT and Shuman BN (2020) Pervasive Desiccation of North American Lakes During the
891 Late Quaternary. *Geophysical Research Letters* 47(3). DOI: 10.1029/2019GL086412.

892 Liefert DT and Shuman BN (2022) Expression of the “4.2 ka event” in the southern Rocky
893 Mountains, USA. *Climate of the Past* 18(5): 1109–1124. DOI: 10.5194/cp-18-1109-2022.

894 Lynch EA (1996) The ability of pollen from small lakes and ponds to sense fine-scale vegetation
895 patterns in the Central Rocky Mountains, USA. *Review of Palaeobotany and Palynology*
896 94(3): 197–210. DOI: 10.1016/S0034-6667(96)00040-1.

897 Mack RN, Rutter NW, Bryant VM, et al. (1978) Reexamination of postglacial vegetation history
898 in northern Idaho: Hager Pond, Bonner Co. *Quaternary Research* 10(2): 241–255. DOI:
899 10.1016/0033-5894(78)90104-7.

900 Mack RN, Rutter NW and Valastro S (1983) Holocene Vegetational History of the Kootenai
901 River Valley, Montana. *Quaternary Research* 20(2): 177–193. DOI: 10.1016/0033-
902 5894(83)90076-5.

903 Mann ME, Bradley RS and Hughes MK (1999) Northern hemisphere temperatures during the
904 past millennium: Inferences, uncertainties, and limitations. *Geophysical Research Letters*
905 26(6): 759–762. DOI: 10.1029/1999GL900070.

906 Marsicek J, Shuman BN, Bartlein PJ, et al. (2018) Reconciling divergent trends and millennial
907 variations in Holocene temperatures. *Nature* 554(7690): 92–96. DOI:
908 10.1038/nature25464.

909 Martin AC and Barkley WD (2000) *Seed Identification Manual*. Caldwell: The Blackburn Press.

910 McAndrews, JH Berti and AA Norris GN (1973) *Key to Quaternary Pollen and Spores of the*

911 Great Lakes Region. Toronto: Royal Ontario Museum Life Sciences Miscellaneous
912 Publication.

913 McWethy D, Alt M, Argiriadis E, et al. (2020) Millennial-Scale Climate and Human Drivers of
914 Environmental Change and Fire Activity in a Dry, Mixed-Conifer Forest of Northwestern
915 Montana. *Frontiers in Forests and Global Change* 3. DOI: 10.3389/ffgc.2020.00044.

916 Mehringer P (1985) Late-quaternary pollen records from the interior Pacific northwest and
917 northern great basin of the United States. In: Bryant Jr. V and Holloway WG (eds.)
918 *Pollen Records of the Late Quaternary North American Sediments*. Dallas: American
919 Association of Stratigraphic Palynologists foundation, pp. 167–189.

920 Mehringer P, Arno S and Petersen K (1977) Postglacial History of Lost Trail Pass Bog,
921 Bitterroot Mountains, Montana. *Arctic and Alpine Research* 9: 345. DOI:
922 10.2307/1550528.

923 Meulendyk T, Moorman BJ, Andrews TD, et al. (2012) Morphology and Development of Ice
924 Patches in Northwest Territories, Canada. *Arctic* 65. Arctic Institute of North America:
925 43–58.

926 Meyer GA, Wells SG and Timothy Jull AJ (1995) Fire and alluvial chronology in Yellowstone
927 National Park: Climatic and intrinsic controls on Holocene geomorphic processes.
928 *Geological Society of America Bulletin* 107(10): 1211–1230. DOI: 10.1130/0016-
929 7606(1995)107<1211:FAACIY>2.3.CO;2.

930 Millspaugh SH, Whitlock C and Bartlein PJ (2000) Variations in fire frequency and climate over
931 the past 17 000 yr in central Yellowstone National Park.: 4.

932 Minckley TA, Shriver RK and Shuman B (2012) Resilience and regime change in a southern
933 Rocky Mountain ecosystem during the past 17 000 years. *Ecological Monographs* 82(1):
934 49–68. DOI: 10.1890/11-0283.1.

935 Morgan C, Losey A and Trout L (2014) Late-Holocene paleoclimate and treeline fluctuation in
936 Wyoming's Wind River Range, USA. *The Holocene* 24(2). SAGE Publications Ltd: 209–
937 219. DOI: 10.1177/0959683613516817.

938 Panshin AJ and de Zeeuw C (1980) *Textbook of Wood Technology*. New York: McGraw-Hill
939 Book Co.

940 Pepin N, Bradley RS, Diaz HF, et al. (2015) Elevation-dependent warming in mountain regions
941 of the world. *Nature Climate Change* 5(5): 5. Nature Publishing Group: 424–430. DOI:
942 10.1038/nclimate2563.

943 Pfister R, Kovalchik B, Arno S, et al. (1977) *Forest habitat types of Montana*. INT-34, General
944 Technical Report. USDA Forest Service.

945 Pierce K, Cannon K, Meyer G, et al. (2002) *Post-glacial inflation-deflation cycles, tilting, and*
946 *faulting in the Yellowstone Caldera based on Yellowstone Lake shorelines*. Open-File
947 Report 02-0142, Open-File Report. US Geological Survey.

948 PRISM Climate Group, Oregon State University (2014). Available at:
949 <https://prism.oregonstate.edu> (accessed 20 Feb 2021).

950 Quadri P, Silva LCR and Zavaleta ES (2021) Climate-induced reversal of tree growth patterns at
951 a tropical treeline. *Science Advances* 7(22): eabb7572. DOI: 10.1126/sciadv.abb7572.

952 Rehm E and Feeley KJ (2016) Many species risk mountain top extinction long before they reach
953 the top. *Frontiers of Biogeography* 8(1). DOI: 10.21425/F5FBG27788.

954 Rust RA and Minckley TA (2020) Fire and hydrologically mediated diversity change in
955 subalpine forests through the Holocene. *Journal of Vegetation Science* 31(3): 380–391.
956 DOI: <https://doi.org/10.1111/jvs.12853>.

957 Schiller CM, Whitlock C and Brown SR (2022) Holocene geo-ecological evolution of Lower
958 Geyser Basin, Yellowstone National Park (USA). *Quaternary Research* 105: 201–217.
959 DOI: 10.1017/qua.2021.42.

960 Schweingruber FH and Landolt W (2005) The Xylem Database. Available at
961 <http://www.wsl.ch/dendropro/xylemdb/index.php?BNAM=Bilder> (accessed 2013-2017).

962 Schwörer C, Gavin DG, Walker IR, et al. (2017) Holocene tree line changes in the Canadian
963 Cordillera are controlled by climate and topography. *Journal of Biogeography* 44(5):
964 1148–1159. DOI: 10.1111/jbi.12904.

965 Shuman B, Henderson AK, Colman SM, et al. (2009) Holocene lake-level trends in the Rocky
966 Mountains, U.S.A. *Quaternary Science Reviews* 28(19–20): 1861–1879. DOI:
967 10.1016/j.quascirev.2009.03.003.

968 Shuman B, Pribyl P, Minckley TA, et al. (2010) Rapid hydrologic shifts and prolonged droughts
969 in Rocky Mountain headwaters during the Holocene: Holocene droughts in the Rocky
970 Mountains. *Geophysical Research Letters* 37(6): n/a-n/a. DOI: 10.1029/2009GL042196.

971 Shuman BN and Marsicek J (2016) The structure of Holocene climate change in mid-latitude
972 North America. *Quaternary Science Reviews* 141: 38–51. DOI:
973 10.1016/j.quascirev.2016.03.009.

974 Shuman BN and Serravezza M (2017) Patterns of hydroclimatic change in the Rocky Mountains
975 and surrounding regions since the last glacial maximum. *Quaternary Science Reviews*
976 173: 58–77. DOI: 10.1016/j.quascirev.2017.08.012.

977 Spaulding SA, Stone JR, Norton SA, et al. (2020) Paleoenvironmental context for the Late
978 Pleistocene appearance of Didymosphenia in a North American alpine lake. *Aquatic
979 Sciences* 82(1): 10. DOI: 10.1007/s00027-019-0681-9.

980 Stone JR, Saros JE and Pederson GT (2016) Coherent late-Holocene climate-driven shifts in the
981 structure of three Rocky Mountain lakes. *The Holocene* 26(7): 1103–1111. DOI:
982 10.1177/0959683616632886.

983 Stuiver M and Reimer PJ (1993) Extended 14C data base and revised CALIB 3.0 14C age
984 calibration program *Radiocarbon* 35: 215-230

985 Thompson RS, Whitlock C, Bartlein PJ, et al. (1993) Climatic changes in Western United States
986 since 18,000 yr BP. In: Wright HE, Kutzbach JE, Web III T, et al. (eds.) *Global Climates
987 Since the Last Glacial Maximum*. Minneapolis: University of Minnesota Press, pp. 468–
988 513.

989 Whitlock C (1993) Postglacial Vegetation and Climate of Grand Teton and Southern
990 Yellowstone National Parks. *Ecological Monographs* 63(2): 173–198. DOI:
991 10.2307/2937179.

992 Whitlock C and Bartlein PJ (1993) Spatial Variations of Holocene Climatic Change in the
993 Yellowstone Region. *Quaternary Research* 39(2): 231–238. DOI:
994 10.1006/qres.1993.1026.

995 Whitlock C, Dean WE, Fritz SC, et al. (2012) Holocene seasonal variability inferred from
996 multiple proxy records from Crevice Lake, Yellowstone National Park, USA.
997 *Palaeogeography, Palaeoclimatology, Palaeoecology* 331–332: 90–103. DOI:
998 10.1016/j.palaeo.2012.03.001.

999 Whitlock C and Larsen C (2001). Charcoal as fire proxy. In: Smol JP, Birks HJB and Last WM
1000 (eds) *Tracking Environmental Change Using Lake Sediments: Terrestrial, Algal, and
1001 Siliceous Indicators*, 3. Dordrecht: Kluwer Academic Publishers, pp. 75–97.

1002 Williams KL (2012) *Classification of the grasslands, shrublands, woodlands, forests and alpine*
1003 *vegetation associations of the Custer National Forest portion of the Beartooth Mountains*
1004 *in southcentral Montana*. PhD Thesis, Montana State University, USA.

1005 Wise EK, Woodhouse CA, McCabe GJ, et al. (2018) Hydroclimatology of the Missouri River
1006 Basin. *Journal of Hydrometeorology* 19(1). American Meteorological Society: 161–182.
1007 DOI: 10.1175/JHM-D-17-0155.1.

1008

1009

1010

1011

1012

1013

1014

1015

1016

1017

1018

1019

1020

1021

1022

1023

1024

1025

1026

1027

1028

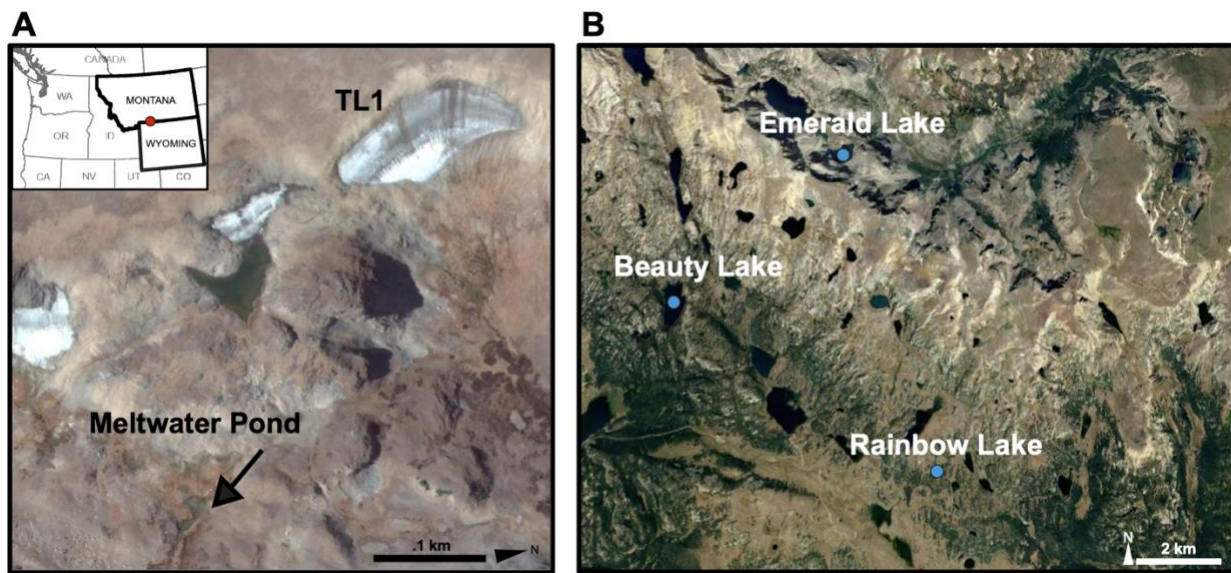
1029

1030

1031

1032

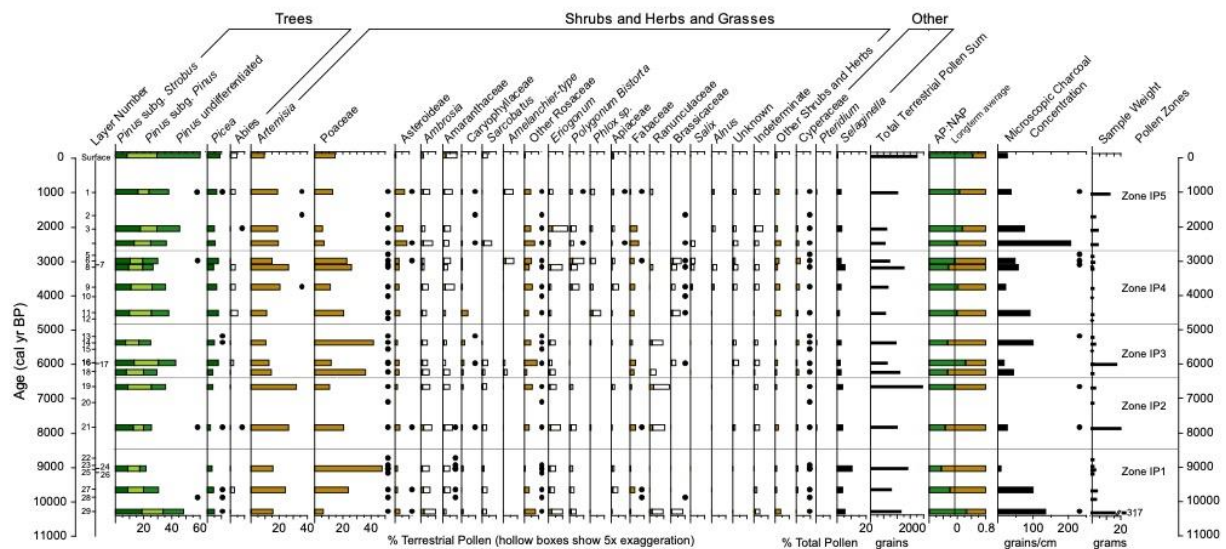
1033 **Figures**



1034

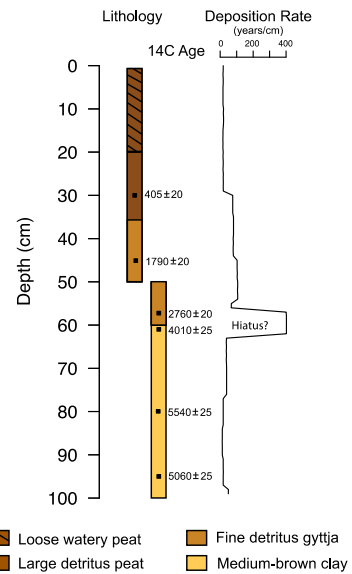
1035 Figure 1A) TL1 Ice Patch and Meltwater Pond. B) Referenced Beartooth Plateau study sites used
 1036 in comparative analyses, within 20 km of TL1: Emerald Lake (Barth et al., 2022), Rainbow Lake
 1037 (Shuman and Serreze, 2017, Rust and Minckley, 2020); Beauty Lake (Spaulding et al., 2020).
 1038 Images from Google Earth.

1039

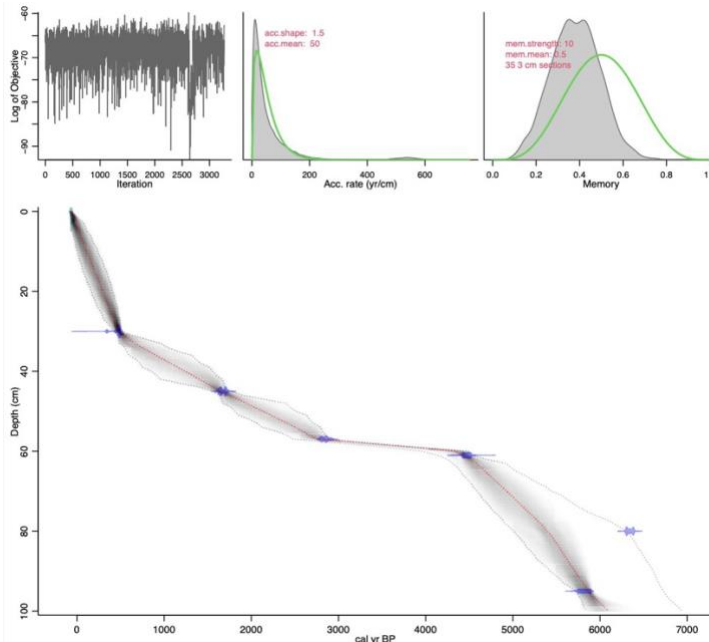


1040

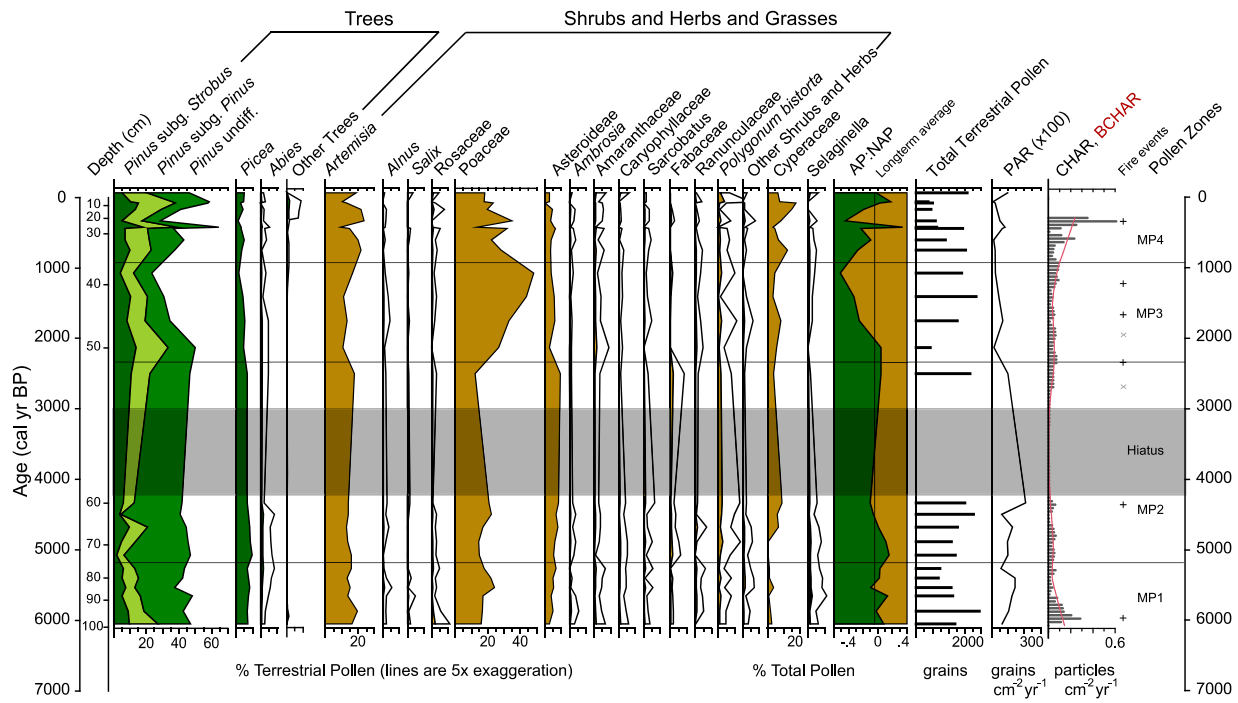
1041 Figure 2. Pollen, macrofossils, and charcoal concentration data from the TL1 Ice Patch. Hollow
 1042 boxes are 5x exaggeration of the pollen percentages for species that never exceed 3%, and circles
 1043 denote the presence of at least one macrofossil. Surface sample is not an organic layer.



1046 Figure 3. Lithology of the Meltwater Pond sediment, location of samples submitted for
 1047 radiocarbon dating, and deposition rate of sedimentation.

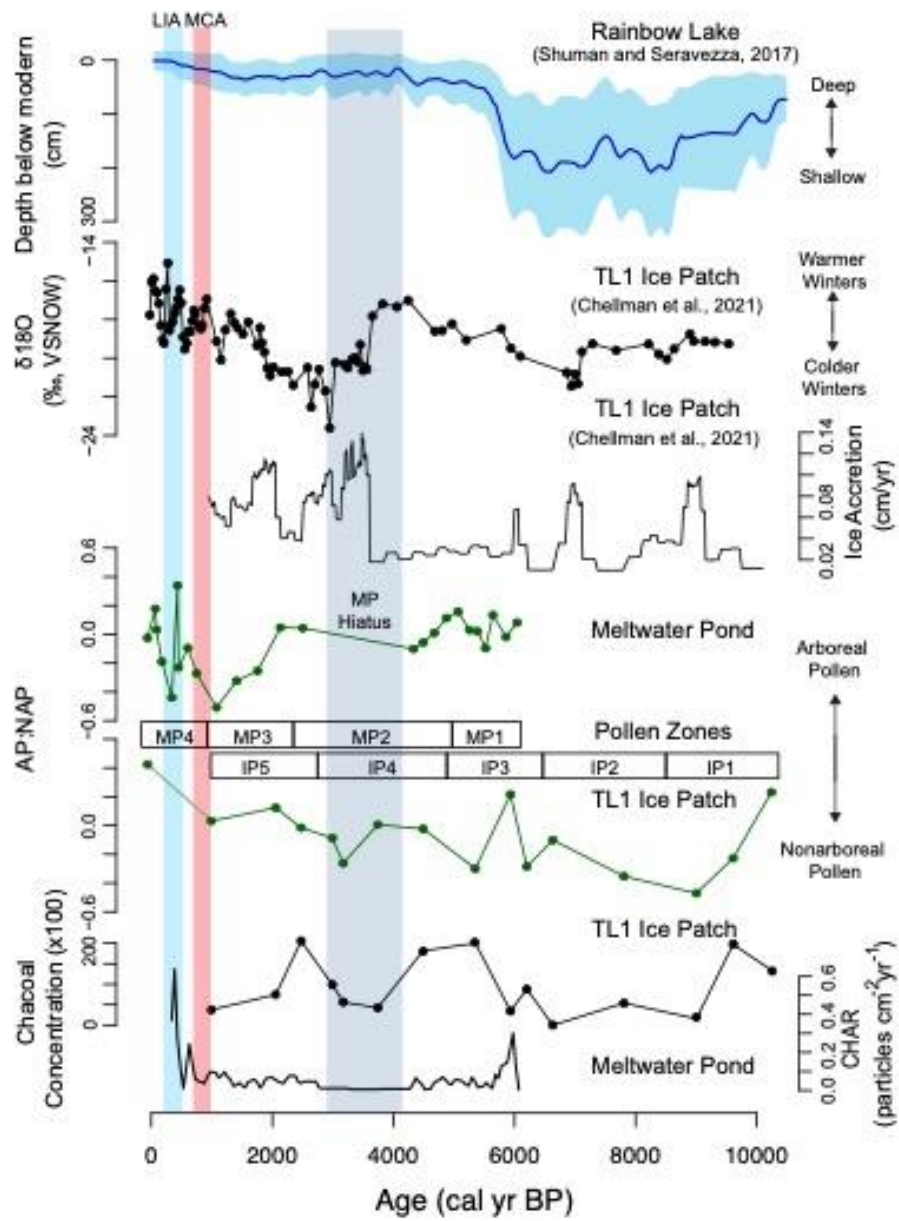


1049 Figure 4. Age-depth model for Meltwater Pond based on six radiocarbon dates.

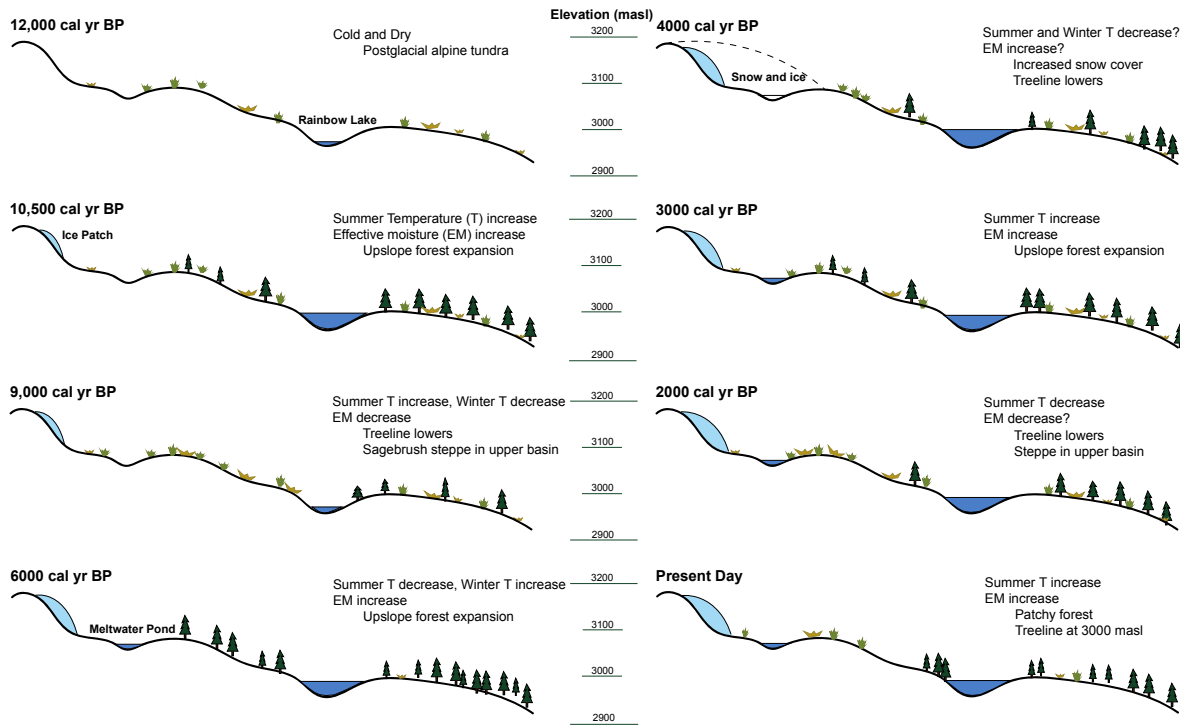


1051

1052 Figure 5. Pollen and charcoal data from Meltwater Pond, WY. Black lines are 5x exaggeration of
 1053 the pollen time series, and (+) symbols denote significant fire events, and (x) symbols indicate
 1054 insignificant fire events.

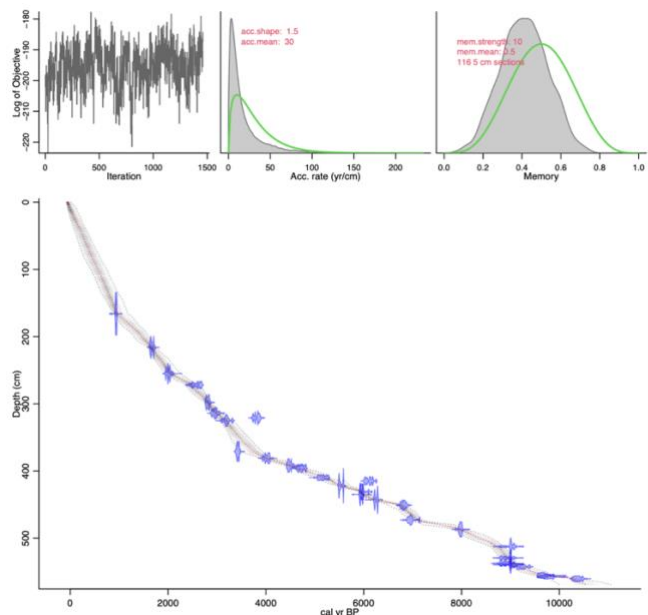


1055
 1056
 1057 Figure 6. Multiproxy comparison of lake level data from Rainbow Lake (Shuman and
 1058 Serravezza, 2017), isotope and ice accumulation data from the TL1 Ice Patch (Chellman et al.,
 1059 2021), the ratio of arboreal to non-arboreal pollen from the TL1 Ice Patch and Meltwater Pond,
 1060 and charcoal data from the TL1 Ice Patch and Meltwater Pond (this study). Pollen zones are
 1061 noted in boxes and TL1 surface arboreal pollen ratio is not from an organic layer.
 1062



1063
1064
1065 Figure 7. Sequence of major paleoenvironmental changes through time on the Beartooth Plateau
1066 based on records from this study and Rainbow Lake studies (Rust and Minckley, 2020; Shuman
1067 and Serravezza, 2017). Changes in temperature and precipitation are relative to the time period
1068 before. Each panel illustrates prominent shifts in vegetation recorded by pollen samples
1069 corresponding to the time period indicated.
1070
1071
1072
1073
1074
1075
1076
1077
1078
1079
1080

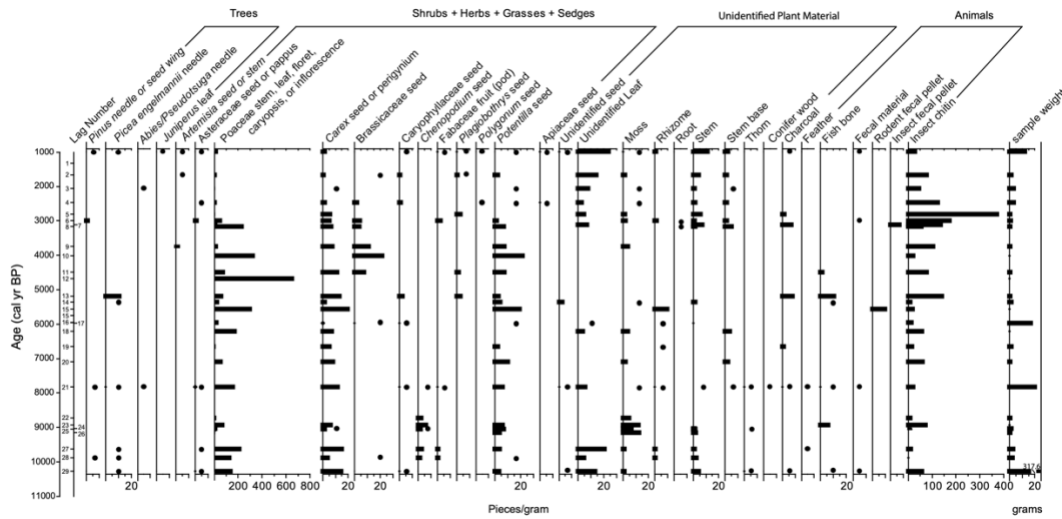
1081 **Supplementary Materials**



1082

1083 SM Fig 1. Age-depth diagram of the TL1 Ice Patch, based on 29 radiocarbon dates.

1084



1085

1086 SM Fig 2. Macrofossils from TL1 Ice Patch organic layers. Dots indicate an amount under 1
1087 piece/gram.

1088

1089